

Kinematic Geometry for the Saddle Line Fitting of Planar Discrete Positions

WU Yu^{1,*}, WANG Delun¹, WANG Wei¹, YU Shudong², and XU Wenji¹

¹ School of Mechanical Engineering, Dalian University of Technology, Dalian 116024, China

² Department of Mechanical and Industrial Engineering, Ryerson University, Toronto, Canada

Received September 18, 2014; revised January 6, 2015; accepted January 19, 2015

Abstract: The position synthesis of planar linkages is to locate the center point of the moving joint on a rigid link, whose trajectory is a circle or a straight line. Utilizing the min-max optimization scheme, the fitting curve needs to minimize the maximum fitting error to acquire the dimension of a planar binary P-R link. Based on the saddle point programming, the fitting straight line is determined to the planar discrete point-path traced by the point of the rigid body in planar motion. The property and evolution of the defined saddle line error can be revealed from three given separate points. A quartic algebraic equation relating the fitting error and the coordinates is derived, which agrees with the classical theory. The effect of the fourth point is discussed in three cases through the constraint equations. The multi-position saddle line error is obtained by combination and comparison from the saddle point programming. Several examples are presented to illustrate the solution process for the saddle line error of the moving plane. The saddle line error surface and the contour map presented to show the variations of the fitting error in the fixed frame. The discrete kinematic geometry is then set up to disclose the relations of the separate positions of the rigid body, the location of the tracing point on the moving body, and the position and orientation of the saddle line to the point-path. This paper presents a new analytic geometry method for saddle line fitting and provides a theoretical foundation for position synthesis.

Keywords: saddle point programming, kinematic geometry, saddle line error, position synthesis

1 Introduction

The position synthesis of planar linkages is to locate the center points of their moving joints, whose trajectories are exactly or approximately circles, or straight lines. The center points can be taken as the moving hinges to construct the required planar linkages. The Burmester theory can be used to determine these characteristic points^[1]. If several positions of a rigid link are prescribed, the relative displacement pole can be introduced to locate the circle point and the Ball point.

BAI^[2] conducted the precision synthesis for a planar four-bar linkage with fewer than five positions, and a planar slider-crank linkage with fewer than four positions by means of the graphical method. The algebraic method has also been employed to establish the constraint equations of a binary link in synthesis of linkages. ROTH^[3-4], SUH, et al^[5], SANDOR, et al^[6], FREUDENSTEIN, et al^[7-10], VELDKAMP^[11] developed the analytical expressions of the Burmester theory for planar motion and extended it to the higher order curvature, which provides the theoretical base for the synthesis of linkages. These

classical works address the following topics: (i) what linkage can trace the desired coupler curves, (ii) the existence of solution to the kinematic synthesis in planar motion with higher order, and (iii) the cognate linkages.

Unfortunately the Burmester theory or the algebraic method is restricted to the position synthesis of planar linkages with the number of the prescribed positions of a rigid link not exceeding five. Naturally, the optimization method is applied to the approximate synthesis of planar linkages. Under the least square premise by AKHRAS et al^[12], the construction error is taken as the objective function; the coordinates of the moving and fixed hinge points are regarded as the optimization variables. ANGELES et al^[13], indicated that min-max optimization is more desirable in mechanism synthesis. LIU, et al^[14], systematically studied the theory of saddle point programming and applied it to the geometric error evaluation. Based on the saddle point programming theory, considerable work has been done on modeling the min-max fitting error^[15-19].

In this paper, a novel geometric approach is proposed to demonstrate how the saddle point theory is used to evaluate the fitting error of a straight line defined by a set of discrete points. The error surface on the moving body evolves with increase in the number of positions of the rigid body. This provides a theoretical basis for solving the optimization problem and the characteristic points yielding

* Corresponding author. E-mail: wuyu1091154038@163.com

Supported by National Natural Science Foundation of China(Grant No. 51275067)

a minimum saddle line error.

2 Error Evaluation and Saddle Line Fitting

The path traced by point P of a rigid link or body in discrete planar movement is represented by a discrete point set $\mathbf{R}_p^{(i)}$ in the fixed frame $\{O_f, i_f, j_f\}$. If a straight line is taken to fit $\mathbf{R}_p^{(i)}$, the normal distance from a point in $\mathbf{R}_p^{(i)}$ to the fitting line is a measure of the fitting error. A straight line, determined by minimizing the maximum fitting error, is defined as the saddle line. The corresponding minimal maximum fitting error is defined as the saddle line error. The saddle line can be sought from the min-max principle or the saddle point programming. A point in $\mathbf{R}_p^{(i)}$ with the maximum fitting error is called as the saddle line fitting-point, or the characteristic point. Points $P^{(1)}$, $P^{(2)}$ and $P^{(3)}$ in Fig. 1 are three characteristic points.

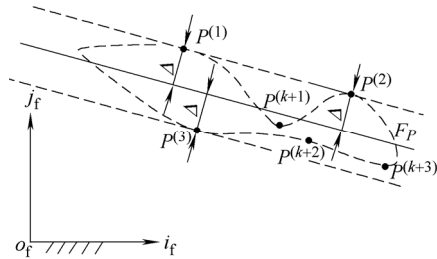


Fig. 1. Points with the extreme normal fitting errors

Based on the saddle point programming, the saddle line of $\mathbf{R}_p^{(i)}$ is determined by a finite number of characteristic points. Once the characteristic points are found, the saddle line error can be obtained through the analytic geometry method. The properties of the saddle line error can be investigated further.

3 Saddle Line of Three Points

Point P of a rigid body has the coordinates (x_{Pm}, y_{Pm}) in the moving Cartesian coordinate system $\{O_m, i_m, j_m\}$. Let $(x_p^{(i)}, y_p^{(i)})$ be a discrete displacement vector of P . The relationship between (x_{Pm}, y_{Pm}) and $(x_p^{(i)}, y_p^{(i)})$ can be represented by the following coordinate transformation:

$$\begin{pmatrix} x_p^{(i)} \\ y_p^{(i)} \\ 1 \end{pmatrix} = \mathbf{M}^{(i)} \cdot \begin{pmatrix} x_{Pm} \\ y_{Pm} \\ 1 \end{pmatrix}, \quad (1)$$

where

$$\mathbf{M}^{(i)} = \begin{pmatrix} \cos \gamma^{(i)} & -\sin \gamma^{(i)} & x_{O_m}^{(i)} \\ \sin \gamma^{(i)} & \cos \gamma^{(i)} & y_{O_m}^{(i)} \\ 0 & 0 & 1 \end{pmatrix}, \quad i = 1, 2, 3.$$

$\mathbf{M}^{(i)}$ is the displacement matrix of the rigid body^[20], $(x_{O_m}^{(i)}, y_{O_m}^{(i)})$ are the coordinates of origin $O_m^{(i)}$ of $\{O_m, i_m, j_m\}$; $\gamma^{(i)}$ is the rotation angle relative to the point $O_m^{(i)}$, shown in Fig. 2.

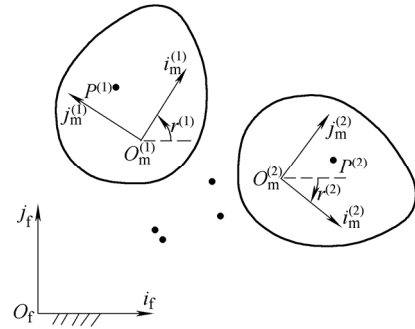


Fig. 2. Moving Cartesian coordinate systems

For geometric error evaluation, the number of characteristic points is three. These points distribute on both sides of the saddle line. It means, the parameter of the saddle line can be determined as long as we find the positions of the three characteristic points.

In the case that three positions, $P^{(1)}$, $P^{(2)}$ and $P^{(3)}$ are the discrete points in the fixed frame traced by the point P , there are totally three cases corresponding to three distributing lines $L_{12,3}$, $L_{13,2}$ and $L_{23,1}$, shown in Fig. 3. These lines have some common properties: the slopes can be obtained by two of the three characteristic points. The fitting error for each distributing line is half of the normal distance from a characteristic point to the distributing line.

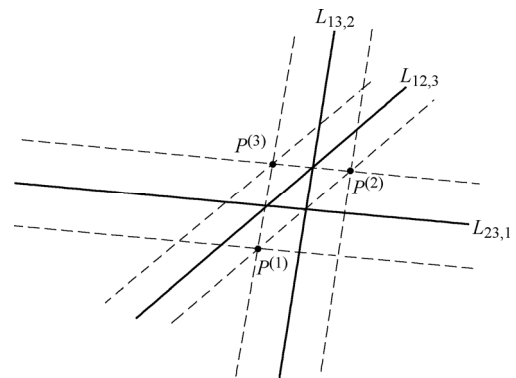


Fig. 3. Three distributing lines based on the three characteristic points

Let line $L_{ij,k}$ and its corresponding fitting error $\Delta_{ij,k}$ represent the distribution case in which points $P^{(i)}$ and $P^{(j)}$ lie on one side of the line, and point $P^{(k)}$ lies on the other side. Then the fitting error $\Delta_{ij,k}$, equals the normal distance from $P^{(i)}$, $P^{(j)}$ or $P^{(k)}$ to $L_{ij,k}$. Take $\Delta_{12,3}$ for example, we have

$$\Delta_{12,3} = \frac{|(\mathbf{R}_p^{(1)} - \mathbf{R}_p^{(2)}) \times (\mathbf{R}_p^{(1)} - \mathbf{R}_p^{(3)})|}{2|\mathbf{R}_p^{(1)} - \mathbf{R}_p^{(2)}|}. \quad (2)$$

The following algebraic equation of the line through points $P^{(1)}$ and $P^{(2)}$ can also be obtained:

$$(x_p^{(2)} - x_p^{(1)})y - (y_p^{(2)} - y_p^{(1)})x + y_p^{(2)}x_p^{(1)} - x_p^{(2)}y_p^{(1)} = 0. \quad (3)$$

The fitting error $\Delta_{12,3}$ may be written as

$$A_{2,3} = \frac{|(x_p^{(2)} - x_p^{(1)})y_p^{(3)} - (y_p^{(2)} - y_p^{(1)})x_p^{(3)} + y_p^{(2)}x_p^{(1)} - x_p^{(2)}y_p^{(1)}|}{2\sqrt{(x_p^{(2)} - x_p^{(1)})^2 + (y_p^{(2)} - y_p^{(1)})^2}} \quad (4)$$

From Eq. (1), the coordinates of points $P^{(1)}$, $P^{(2)}$ and $P^{(3)}$ can be obtained and then substituted into the above equation. We may obtain the following quartic algebraic equation, which implies the relationship between x_{Pm} , y_{Pm} and $\Delta_{12,3}$, that is

$$4(a_1x_{Pm}^2 + a_1y_{Pm}^2 + a_2x_{Pm} + a_3y_{Pm} + a_4)\Delta_{2,3}^2 - (a_5x_{Pm}^2 + a_5y_{Pm}^2 + a_6x_{Pm} + a_7y_{Pm} + a_8)^2 = 0, \quad (5)$$

where

$$\begin{cases} a_1 = 2 - 2\cos(\gamma^{(2)} - \gamma^{(1)}), \\ a_2 = 2(x_{Om}^{(2)} - x_{Om}^{(1)})(\cos\gamma^{(2)} - \cos\gamma^{(1)}) + 2(y_{Om}^{(2)} - y_{Om}^{(1)})(\sin\gamma^{(2)} - \sin\gamma^{(1)}), \\ a_3 = 2(x_{Om}^{(2)} - x_{Om}^{(1)})(\sin\gamma^{(1)} - \sin\gamma^{(2)}) + 2(y_{Om}^{(2)} - y_{Om}^{(1)})(\cos\gamma^{(2)} - \cos\gamma^{(1)}), \\ a_4 = (x_{Om}^{(2)} - x_{Om}^{(1)})^2 + (y_{Om}^{(2)} - y_{Om}^{(1)})^2, \\ a_5 = \sin(\gamma^{(1)} - \gamma^{(2)}) + \sin(\gamma^{(2)} - \gamma^{(3)}) + \sin(\gamma^{(3)} - \gamma^{(1)}), \\ a_6 = (x_{Om}^{(1)} - x_{Om}^{(2)})\sin\gamma^{(3)} + (x_{Om}^{(2)} - x_{Om}^{(3)})\sin\gamma^{(1)} + (x_{Om}^{(3)} - x_{Om}^{(1)})\sin\gamma^{(2)} + (y_{Om}^{(2)} - y_{Om}^{(1)})\cos\gamma^{(3)} + (y_{Om}^{(3)} - y_{Om}^{(2)})\cos\gamma^{(1)} + (y_{Om}^{(1)} - y_{Om}^{(3)})\cos\gamma^{(2)}, \\ a_7 = (x_{Om}^{(1)} - x_{Om}^{(2)})\cos\gamma^{(3)} + (x_{Om}^{(2)} - x_{Om}^{(3)})\cos\gamma^{(1)} + (x_{Om}^{(3)} - x_{Om}^{(1)})\cos\gamma^{(2)} + (y_{Om}^{(1)} - y_{Om}^{(2)})\sin\gamma^{(3)} + (y_{Om}^{(2)} - y_{Om}^{(3)})\sin\gamma^{(1)} + (y_{Om}^{(3)} - y_{Om}^{(1)})\sin\gamma^{(2)}, \\ a_8 = (y_{Om}^{(2)} - y_{Om}^{(1)})x_{Om}^{(3)} + (y_{Om}^{(3)} - y_{Om}^{(2)})x_{Om}^{(1)} + (y_{Om}^{(1)} - y_{Om}^{(3)})x_{Om}^{(2)}. \end{cases}$$

Errors $\Delta_{23,1}$ of $L_{23,1}$ and $\Delta_{13,2}$ of $L_{13,2}$ can be obtained in a similar way. The three-points saddle line error Δ of the set $R_p^{(i)}$ ($i=1, 2, 3$) is the minimum of the three distributing line errors, or

$$\Delta = \min(\Delta_{12,3}, \Delta_{13,2}, \Delta_{23,1}). \quad (6)$$

The above relation may be written as follows:

$$\Delta = \frac{\left| \frac{|A_{23,1} + A_{13,2}|}{2} - \frac{|A_{23,1} - A_{13,2}|}{2} \right| + A_{12,3}}{2} - \frac{\left| \frac{|A_{23,1} + A_{13,2}|}{2} - \frac{|A_{23,1} - A_{13,2}|}{2} \right| - A_{12,3}}{2}. \quad (7)$$

For a point in the moving Cartesian coordinate frame, the saddle line error can be derived from Eq. (7) with the given parameters $\gamma^{(i)}$, $x_{Om}^{(i)}$, $y_{Om}^{(i)}$, of the three positions. Meanwhile,

considering the symmetry of the coefficients a_5 - a_8 in Eq. (6), if $\Delta_{12,3}$, $\Delta_{13,2}$ and $\Delta_{23,1}$ equal zero at the same time, the three quartic algebraic equations yield a single sliding point circle, consistent with the Burmester theory.

4 Change Incurred by the Fourth Point

For the four separate positions, point P traces a planar discrete point set $R_p^{(i)}$ ($i=1, 2, 3, 4$), which comprises four points, $P^{(1)}$, $P^{(2)}$, $P^{(3)}$ and $P^{(4)}$. The saddle line obtained by saddle point programming is called a four-point saddle line. When the fourth discrete point $P^{(4)}$ is added, the relationship between the three-points saddle line and four-points saddle line needs to be established. Depending upon the position of $P^{(4)}$, it is discussed in three cases. To facilitate discussion, we assume that $L_{12,3}$ is the three-point saddle line and $\Delta_{12,3}$ is the saddle line error.

Case 1. The fourth point $P^{(4)}$ is not a characteristic point; the saddle line does not change.

If $P^{(4)}$ lies in the containing area by the parallel dotted line of $L_{12,3}$ (it is called as “the parallel area of $L_{12,3}$ ” for short in the following paragraphs), it is obvious that the first three points $P^{(1)}$, $P^{(2)}$ and $P^{(3)}$ are still characteristic points, which meets the first case.

If $P^{(4)}$ is out of the parallel area, it should be the point with the maximum error if $L_{12,3}$ is the four-point saddle line, which is in contradiction with the hypothesis. As a result, $P^{(4)}$ needs to meet the following inequalities to indicate the parallel area of $L_{12,3}$:

$$\begin{cases} (R_p^{(1)} - R_p^{(2)}) \times (R_p^{(1)} - R_p^{(4)}) < (R_p^{(1)} - R_p^{(2)})(R_p^{(1)} - R_p^{(3)}), \\ (R_p^{(1)} - R_p^{(2)}) \times (R_p^{(3)} - R_p^{(4)}) < (R_p^{(1)} - R_p^{(2)})(R_p^{(1)} - R_p^{(3)}). \end{cases} \quad (8)$$

Case 2. The fourth point $P^{(4)}$ is not the characteristic point; the saddle line changes. That is to say, $P^{(1)}$, $P^{(2)}$ and $P^{(3)}$ are still characteristic points, while the four-points saddle line transforms from $L_{12,3}$ to $L_{13,2}$ or $L_{23,1}$. Take the situation that $L_{12,3}$ changes to $L_{13,2}$ for instance, the requirement $P^{(4)}$ needs to meet is discussed in further detail below.

Any three of the four points $P^{(i)}$ ($i=1, 2, 3, 4$) can be grouped together to obtain three fitting lines. It means, there are $C_4^3 \times 3 = 12$ distributing lines in total. Define $\Delta_{ij,k}^{(n)}$ as the distance of the n -th point $P^{(n)}$ to $L_{ij,k}$, and $\Delta_{ij,k}^M$ as the maximum value of the set $\Delta_{ij,k}^{(n)}$ ($n=1, 2, 3, 4$). Each distributing line corresponds to one $\Delta_{ij,k}^M$ according to the subscript of $L_{ij,k}$ while there are 12 $\Delta_{ij,k}^M$ in total. When the saddle line changes from $L_{12,3}$ to $L_{13,2}$, it is obvious that all $\Delta_{ij,k}^M$ need to be greater than the saddle line error $\Delta_{13,2}$ except $\Delta_{13,2}^M$. There are two conditions that $P^{(4)}$ needs to satisfy at the same time.

Condition 1: For $\Delta_{13,2}^M$, that is

$$\Delta_{13,2}^M = \Delta_{13,2}. \quad (9)$$

Condition 2: For the other 11 $\Delta_{ij,k}^M$, that is

$$\{\Delta_{ij,k}^M > \Delta_{3,2}\}. \tag{10}$$

$$\Delta_{23,1}^M = \Delta_{23,1}, \tag{11}$$

$$\{\Delta_{ij,k}^M > \Delta_{23,1}\}. \tag{12}$$

From the geometric approach, Eq. (9) means that $P^{(4)}$ is in the parallel area of $L_{13,2}$, while the equation set in Eq. (10) means that $P^{(4)}$ is in the intersection of the 11 areas corresponding to the 11 equations.

In a similar way, when the saddle line changes from $L_{12,3}$ to $L_{23,1}$, we also have an equation and an equation set, that is

Case 3. The fourth point $P^{(4)}$ is one of the three characteristic points; the saddle line changes. Apparently, $P^{(4)}$ will meet case 3 so long as the point dissatisfies cases 1 and 2. Fig. 4 shows the three different cases discussed and illustrate the relationship between the position and the effect of the fourth point.

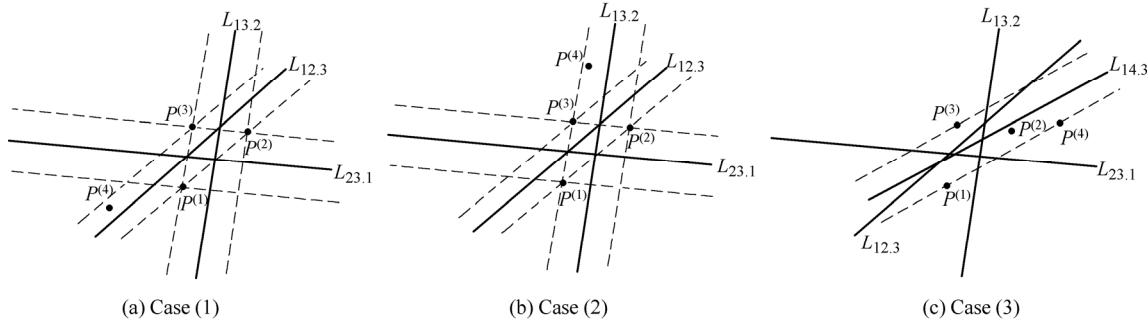


Fig. 4. Three cases incurred by the fourth point

5 Solution for Saddle Line Error of Multi-points

From sections 3 and 4, the way to find the multi-point saddle line can be concluded. For multiple positions, point P traces a planar discrete point set $R_p^{(i)} (i=1, 2, 3, \dots, n)$. Any three of the discrete points can be grouped together to obtain three distributing lines and three fitting errors. There are C_n^3 groups in total. If the other discrete points are in the parallel area of a fitting line, the fitting error is a valid error, otherwise, an invalid error.

For example, there are three distributing lines $L_{12,3}$, $L_{13,2}$ and $L_{23,1}$, three fitting errors $\Delta_{12,3}$, $\Delta_{13,2}$ and $\Delta_{23,1}$ with the group consists of $P^{(1)}$, $P^{(2)}$ and $P^{(3)}$. If all the other discrete points $P^{(1)}-P^{(n)}$ are in the parallel area of $L_{12,3}$, the corresponding fitting error $\Delta_{12,3}$ is a valid error. On the other hand, so long as one discrete point of $P^{(1)}-P^{(n)}$ lies out of the parallel area, $\Delta_{12,3}$ is an invalid error.

In this way, $3 \times C_n^3$ fitting errors from the multi-points are obtained. The number of valid errors can be one or more based on the positions of the points. According to the definition of the saddle line error, the line which can make the maximum fitting error minimum needs to be revealed, so the minimum of the valid errors is apparently the multi-points saddle line error corresponding to the saddle line.

6 Numerical Examples

To validate the theory of saddle line error, a rigid body with three positions, four positions and ten positions is

studied as numeral examples.

6.1 Three positions

As the parameters are defined by the first three positions in Table 1, the saddle line error of any point in the rigid body can be solved by the coordinate transformation matrix introduced in section 3. With the coordinates (x_{Pm}, y_{Pm}) as the independent variables and the three-points saddle line error Δ_{123} as the function value, the error surface and the contour map are depicted by matlab^[21], shown in Fig. 5 and Fig. 6.

Table 1. Ten separated positions of the rigid body in planar movement

Position No.	x_{om}^i	y_{om}^i	$\gamma^i / (^\circ)$
1	0	0	0
2	1.5	0.8	10
3	1.6	1.5	20
4	2.0	3.0	60
5	3.0	3.5	80
6	4.5	5.0	90
7	5.0	5.2	120
8	7.5	6.4	150
9	9.0	7.5	160
10	12.0	8.8	180

Fig. 5 shows the saddle line error of any point in the moving plane and Fig. 6 shows the variation trend of the error. In particular, if the saddle line error is zero, there is an intersection curve of the error surface and the plane defined by $\Delta=0$. The circular curve is the sliding point circle according to the definition, shown in Fig. 6 with the thick line.

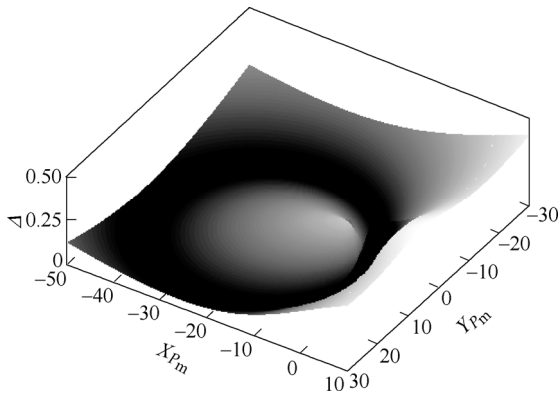


Fig. 5. Saddle line error surface with three positions

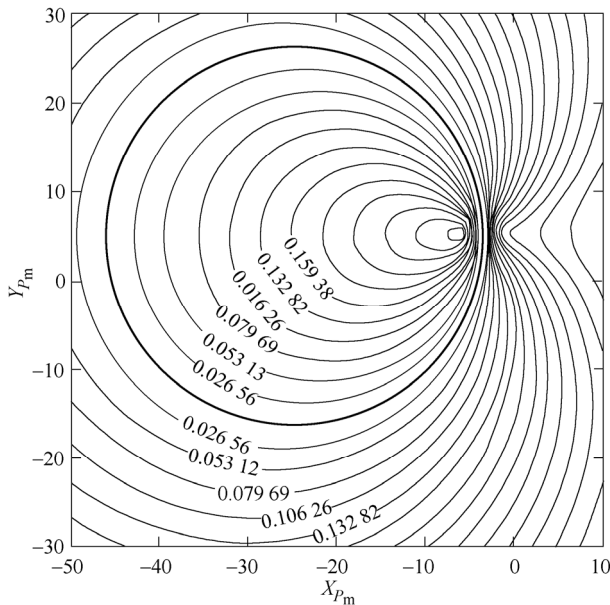


Fig. 6. Contour map with three positions

6.2 Four positions

As to the first four separate positions listed in Table 1, the moving plane is divided into three types of areas based on the different impact incurred by the fourth point, shown in Fig. 7. Consistent with the three cases discussed in section 4, when point P is in area A, the first three-points saddle line is the same as the four-points saddle line, corresponding to case(1); When P is in area B, the four-points saddle line changes but the three characteristic points are still $P^{(1)}$, $P^{(2)}$ and $P^{(3)}$, corresponding to case(2); When P is in area C, $P^{(4)}$ becomes one of the characteristic points, as the saddle line error is defined by $P^{(4)}$ and any two of the first three points, corresponding to case(3).

Similarly to the three separate positions, the contour map of the saddle line error surface with four positions are constructed and shown in Fig. 8. Based on the different groups of the characteristic points, the moving plane can be separated into four parts from I to IV. Part I corresponds to the group with the characteristic points $P^{(1)}$, $P^{(2)}$ and $P^{(3)}$, part II to 124, part III to 134 and part IV to 234. Particularly, when P lies at the intersection point of the four parts (the black dot in Figure 8, the four discrete points $P^{(1)}-P^{(4)}$ need

to meet the requirement of all the four parts at the same time, which means the four points are collinear and the saddle line error is zero. The intersection point was defined as the sliding point in classical theory. The conclusion can also be verified according to the variation trend of contour lines.

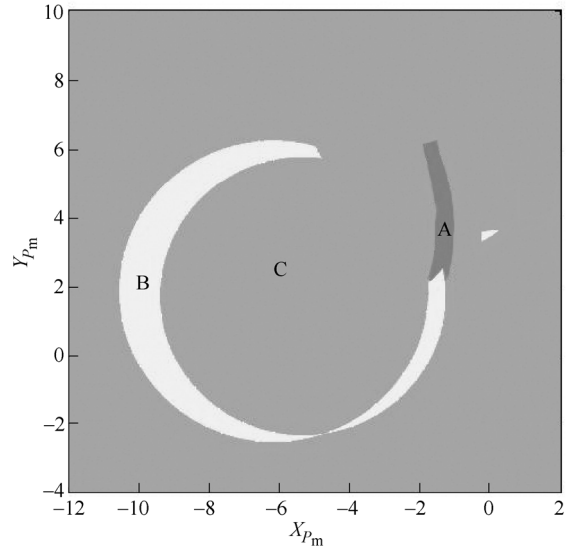


Fig. 7. Areas based on the three cases

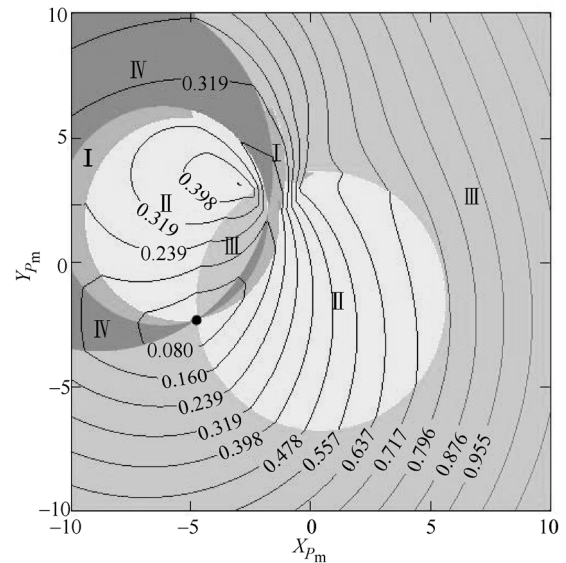


Fig. 8. Four-position saddle line errors with different parts

6.3 Ten positions

For the ten separated positions listed in Table 1, the error surface is depicted by combination and comparison, shown in Fig. 9.

In a way to similar to the four positions, the error surface consists of several quartic surfaces corresponding to different three-point groups can be constructed.

7 Conclusions

- (1) The fitting straight line with the three characteristic points is determined for the planar discrete points traced by

a moving body. Based on the saddle point programming, a new analytic geometry method for saddle line fitting is developed. The saddle line error is solved with three separate points and the effect of the fourth point is discussed in three cases. The analysis agrees with the Burmester theory for fewer than four given positions.

(2) By combination and comparison, the way for the multi-point saddle line error is revealed. Several examples are presented to illustrate the error of a point in the rigid body with saddle line error surface of the moving plane.

(3) Based on the saddle line error surface with several discrete positions, the point which corresponds to the minimum fitting error of the moving body needs to be searched. It is necessary to find the boundaries of the different parts corresponding to the different three-point groups, while the minimum fitting error for all parts can be solved

(4) The discrete kinematic geometry is set up to disclose the relations of the separated positions of the rigid body. It provides a theoretical foundation for the position synthesis of planar binary P-R link, and the solution of saddle line error in the paper can be extended in many other open kinematic chains like planar binary R-R link and spatial binary S-S link.

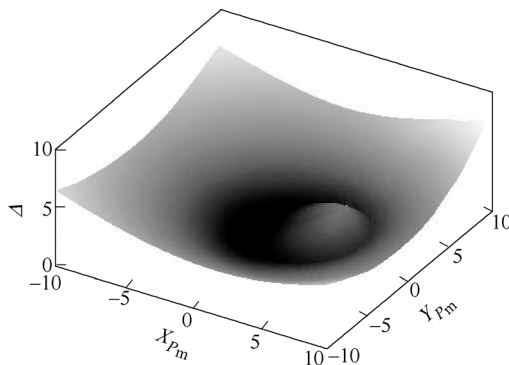


Fig. 9. Saddle line error surface with ten positions

References

- [1] BURMESTER L. *Lehrbuch der Kinematik*[M]. Felix, Leipzig, 1888.
- [2] BAI S X. *Advanced mechanism*[M]. Shanghai: Shanghai Scientific and Technical Publishers, 1988. (in Chinese)
- [3] ROTH B. On the screw axes and other special lines associated with spatial displacements of a rigid body[J]. *Journal of Manufacturing Science and Engineering*, 1967, 89(1): 102–110.
- [4] ROTH B. On the multiple generation of coupler-curves[J]. *Journal of Manufacturing Science and Engineering*, 1965, 87(2): 177–183.
- [5] SUH C H, RADCLIFFE C W. *Kinematic and mechanisms design*[M]. New York: John Wiley & Sons, 1978.
- [6] SANDOR G N, FREUDENSTEIN F. Higher-Order plane motion theories in kinematic synthesis[J]. *Journal of Manufacturing Science and Engineering*, 1967, 89(2): 223–230.
- [7] FREUDENSTEIN F, SANDOR G N. On the Burmester points of a plane[J]. *Journal of Applied Mechanics*, 1961, 28(1): 41–49.
- [8] FREUDENSTEIN F. On the variety of motions generated by mechanisms[J]. *Journal of Manufacturing Science and Engineering*, 1962, 84(1): 156–159.
- [9] FREUDENSTEIN F, PRIMROSE E J F. Geared five-bar motion: Part I—Gear ratio minus one[J]. *Journal of Applied Mechanics*, 1963, 30(2): 161–169.
- [10] FREUDENSTEIN F. Higher path-curvature analysis in plane kinematics[J]. *Journal of Manufacturing Science and Engineering*, 1965, 87(2): 184–190.
- [11] VELDKAMP G R. Some remarks on higher curvature theory[J]. *Journal of Manufacturing Science and Engineering*, 1967, 89(1): 84–86.
- [12] AKHRAS R, ANGELES J. Unconstrained nonlinear least-square optimization of planar linkages for rigid-body guidance[J]. *Mechanism and Machine Theory*, 1990, 25(1): 97–118.
- [13] ANGELES J, ALIVIZATOSS A, AKHRAS R. An unconstrained nonlinear least-square method of optimization of RRRR planar path generators[J]. *Mechanism and Machine Theory*, 1988, 23(5): 343–353.
- [14] LIU J, WANG X M. *Saddle point programming and geometric error evaluation*[M]. Dalian: Dalian University of Technology Press, 1996. (in Chinese)
- [15] WANG S F. *New Approach for kinematic synthesis of mechanism by adaptive curve fitting*[D]. Dalian University of Technology, 2005. (in Chinese)
- [16] WANG D L, WANG S F, Li T. Kinematic synthesis of the planar four-bar linkage by adaptive curve fitting[J]. *Journal of Mechanical Engineering*, 2001, 37(12): 21–26. (in Chinese)
- [17] WANG D L, XIAO D Z. Distribution of coupler curves for crank-rocker linkages[J]. *Mechanism and Machine Theory*, 1993, 28(5): 671–684.
- [18] WANG D L, XIAO D Z, LIU J. Ball's curve and Burmester's curve for four-bar linkage[J]. *Journal of Dalian University of Technology*, 1994, 34(4): 411–417. (In Chinese)
- [19] LAN Z H, ZOU H J. Parallel optimization of mechanisms based on the local characteristics of the coupler curves [J]. *Journal of Mechanical Engineering*, 1999, 35(5): 16–19. (in Chinese)
- [20] WANG D L, GAO Y. *Mechanism and machine theory*[M]. Beijing: China Machine Press, 2011. (in Chinese)
- [21] XUE S. *Course of Matlab*[M]. Beijing: Tsinghua University press, 2011. (in Chinese)

Biographical notes

WU Yu, born in 1991, is currently a PhD candidate at *Dalian University of Technology, China*. He received his bachelor degree from *Dalian University of Technology, China*, in 2013. His research interests include mechanisms analysis and synthesis. Tel: +86-152-41466432; E-mail: wuyu1091154038@163.com

WANG Delun, born in 1958, is currently a professor and a PhD candidate supervisor at *Dalian University of Technology, China*. He received his PhD degree from *Dalian University of Technology, China*, in 1995. E-mail: dlunwang@dlut.edu.cn

WANG Wei, born in 1985, is currently a PhD candidate at *Dalian University of Technology, China*. E-mail: wangweidlut@mail.dlut.edu.cn

YU Shudong, born in 1962, is currently a professor of mechanical engineering at *Ryerson University, Toronto, Canada*. He received his PhD degree from *University of Toronto* in 1995. E-mail: syu@ryerson.ca.

XU Wenji, born in 1964, is currently a professor and a PhD candidate supervisor at *Dalian University of Technology, China*. He received his PhD degree from *Dalian University of Technology, China*, in 2000. E-mail: wenjixu@163.com